

LATCHING CONTROL FOR THE POINT-ABSORBER

WAVE-POWER DEVICE

Ruth E. Hoskin & Nancy K. Nichols

Department of Mathematics, University of Reading

NUMERICAL ANALYSIS REPORT 1/86

KEYWORDS: wave-power, wave-energy, optimal control,
phase control, latching.

C O N T E N T S

	<u>Page</u>
Abstract	1
1. Introduction	2
2. Mathematical Model	4
2.1 Problem Formulation	4
2.2 Necessary Conditions for the Optimal	7
2.3 Existence of the Optimal	9
2.4 Lagrange Formulation	11
3. Numerical Methods	14
3.1 Iterative Methods	14
3.2 Discretization of Scheme	21
4. Results	24
Tables 1(a) and 1(b)	29
Tables 2 and 3	30
Tables 4 and 5	31
5. Conclusions	32
6. References	34
Appendix I	35
Graphs : Figure 1	36
Figure 2	37
Figure 3	38
Figure 4	39
Figure 5	40
Figure 6	41
Acknowledgements	42

ABSTRACT

We investigate the use of optimal control techniques for analysing the problem of energy extraction from a simple wave-power device. A mathematical model of the system is developed, and an optimal control strategy for power generation is determined. Various algorithms are considered for solving the problem, and the results obtained show that it is possible to achieve an increase in the power extracted from the device by means of a suitable control strategy. The technique is applicable to irregular, as well as regular, waves.

1. INTRODUCTION

Methods for the generation of power from renewable sources, such as wave, wind, tidal, solar and geothermal energy, have recently received much attention. Investigation has generally concentrated on the modelling of interactions between the devices and power sources and on the analysis of energy-absorption under idealised conditions [Evans (1976), Count (1982)]. Incorporation of a power-conversion system into these designs had led to the development of devices which are sub-optimal from a theoretical point of view - with an energy-capture less than ideal. In this paper we investigate the use of control mechanisms for improving the efficiency of the power-conversion system in a particular wave-power device. With such mechanisms the delivered cost of the energy is reduced, at the expense of a (hopefully) modest increase in capital investment, and wave-power can be made more attractive.

A simple one-dimensional (scalar) model of a damped oscillatory device with a harmonic forcing function is studied [Budal, Falnes et al (1982)], the objective being to control the spring system so as to maximise the power generated by the device over a given time-interval. It has been recognised [Budal and Falnes (1978)] that the explanation for the reduced energy absorption achieved by early designs lies in the relative phase difference between the device motion and the wave-exciting force. For a small device, with a higher natural frequency than the incident wave force, the velocity of the device leads the wave in phase. For a single point-absorber device it has been demonstrated that if the motion of the device is halted for certain periods of time during the wave-cycle, then a more advantageous phase-relationship can be obtained, with a subsequent increase in energy capture [Evans (1976)]. Thus the optimal control is non-linear with discontinuities at switches which are to be determined. Techniques

developed by Birkett (1980); Birkett, Count and Nichols (1984) and Birkett and Nichols (1983) in an investigation into the use of optimal control techniques for analysing the problem of energy extraction from tidal flows, are extended to our problem of wave-power generation.

The problem is formulated mathematically in section 2. The dynamic behaviour of the device is described by a second-order system of ordinary differential equations, which determine the motion of the device. A control variable is introduced to represent the clamping of the device. The problem is to determine the control which maximises the energy produced by the system, subject to the dynamic equations being satisfied, and certain constraints on the control. Necessary conditions for the solution are derived using optimal control theory, and properties of the optimal solution are developed. The numerical procedures considered for determining the optimal control strategy are described in Section 3, and the convergence and stability properties of each are investigated. The results obtained by implementing each algorithm are presented in Section 4, and finally the conclusions drawn from this study are discussed in Section 5. It is demonstrated that, for irregular waves, phase-control of the point absorber device is feasible and that energy-capture can be significantly increased by applying a control in the power-conversion system.

2. MATHEMATICAL MODEL

2.1 Problem Formulation

One simple model for a wave-power device is that of a one-dimensional damped oscillating system with a harmonic forcing function. The main body of the device consists of a freely floating buoy constrained to move in a vertical direction on a strut which is fixed to the sea-bed. If uncontrolled, the buoy oscillates with the motion of the incident wave. However, by clamping the buoy to the strut during controlled intervals of time, it is possible to obtain maximum amplitude oscillations and, hence, maximum power may be extracted from the device.

In the absence of hydrodynamic and mechanical damping, the buoy oscillates with harmonic motion. The vertical displacement, $x(t)$, of the buoy obeys the following second-order differential equation:

$$m\ddot{x} + (k+c)\dot{x} + p^2x = f(t) \quad , \quad (2.1)$$

with $p^2 > \left(\frac{k+c}{2}\right)^2$. Here $f(t)$ represents the motion of the incident wave, assumed to be harmonic; m is the mass associated with the system; k and c are the hydrodynamic and energy-associated damping coefficients respectively and p a spring constant. All constants m, p, k, c are positive quantities, and for convenience we assume $m = 1$. Clamping the device is modelled by applying an additional damping force of large magnitude.

The energy, E , which can be extracted from the device over a time interval $[0, T]$, is given by

$$E = \int_0^T c \dot{x}^2 dt. \quad (2.2)$$

If we examine the solution to equation (2.1), we can see that the solution of the homogeneous equation decays to zero in time if the damping term $(k+c)$ is positive. Thus, if $k + c > 0$, the periodic solution to (2.1) will be equal to the particular integral only. For a harmonic forcing

function of the form $f = e^{i\omega t}$, the periodic solution can be shown to be

$$x(t) = \frac{e^{i\omega t}}{(p^2 - \omega^2) + i\omega(k+c)} \quad (2.3)$$

and the associated energy functional is therefore given by

$$E = \frac{c\omega^2 T}{2[(p^2 - \omega^2)^2 + \omega^2(k+c)^2]} \quad (2.4)$$

Clearly, energy-capture will be maximised if the natural device frequency p is equal to the forcing frequency ω . In this case we obtain

$$E = \frac{cT}{2(k+c)} \quad (2.5)$$

which is maximised with respect to d if the device is 'optimally damped', that is if the energy-associated damping c is set equal to the hydrodynamic damping k . The latching problem is then defined as follows : Determine the partition

$$\pi_N : 0 = t_0 < t_1 < \dots < t_N = T$$

of the interval $[0, T]$, which maximises E over all π_N (for any N), subject to

$$\ddot{x} + (k+c)\dot{x} + p^2x = f(t) \quad \text{for } t \in [t_j, t_{j+1}], j \in J \quad (2.6)$$

and $\dot{x} = 0$ for $t \in [t_j, t_{j+1}], j \notin J$,

where J is any subset of the integers $\{0, 1, 2, \dots, N-1\}$, and where some initial or boundary conditions are imposed upon the state, $x(t)$.

In order to reformulate the above as a standard problem of optimal control, we first introduce a scalar control function $u(t)$ and model the overall behaviour of the system by the single equation

$$\ddot{x} + [(k+c) + uG]\dot{x} + p^2x = f(t) \quad , \quad (2.7)$$

where $G \gg 1$, $(k+c)$, p^2 and $u(t) \in [0,1] \forall t$. When the control is 'off' ($u=0$), the motion satisfies equation (2.1), but when it is 'on' ($u=1$), the motion is approximately $\dot{x} = 0$, with greater accuracy being achieved by taking a larger value for G . We rewrite the second-order differential equation as the first-order system:

$$\dot{x}(t) = v(t) \quad (2.8)$$

$$\dot{v}(t) = f(t) - p^2x(t) - [(k+c) + u(t)G]v(t) \quad . \quad (2.9)$$

The control problem is thus to

$$\text{maximise } E = \int_0^T \underline{x}^T C \underline{x} dt \quad (2.10)$$

$$\text{subject to } \dot{\underline{x}} = A\underline{x} + uB\underline{x} + \underline{b} \quad (2.11)$$

$$\text{and either (i) } \underline{x}(0) = \underline{x}_0, \text{ given} \quad (2.12)$$

$$\text{or (ii) } \underline{x}(0) = \underline{x}(T) \quad , \quad (2.13)$$

where T is given and

$$\underline{x} = \begin{bmatrix} x \\ v \end{bmatrix}, \quad A = \begin{bmatrix} 0 & 1 \\ -p^2 & -(k+c) \end{bmatrix}, \quad B = \begin{bmatrix} 0 & 0 \\ 0 & -G \end{bmatrix}, \quad C = \begin{bmatrix} 0 & 0 \\ 0 & c \end{bmatrix}, \quad \underline{b} = \begin{bmatrix} 0 \\ f(t) \end{bmatrix} \quad .$$

Admissible controls are those belonging to the set D of measurable functions on $[0,T]$ satisfying

$$u(t) \in \Omega = [0,1], \quad \forall t \in [0,T] \quad , \quad (2.14)$$

where Ω is termed the restraint set. We observe that imposing boundary condition (2.13) results in a periodic solution.

It is not immediately apparent that the problem defined by (2.10)-(2.14) is equivalent to the original problem (2.6), since the control is allowed to take values over the entire interval $[0,1]$. However, in the following section, necessary conditions derived for the solution show the optimal control to be of a "bang-bang" nature, taking values only at the boundaries

of the restraint set. Hence the problems are equivalent.

2.2 Necessary Conditions for the Optimal

In order to establish the optimal control for the problem (2.10)-(2.14) we apply the following Maximum Principle (Pontryagin et al. [1962], Lee and Markus [1967]):

Theorem

For a control u , with corresponding state \underline{x} , satisfying (2.11)-(2.13), to be an optimal solution, it is necessary that there exists a continuous vector $\underline{\lambda}(t) : [0, T] \rightarrow \mathbb{R}^2$, called the adjoint variable, such that if the Hamiltonian, H , is defined by

$$H = \underline{x}^T C \underline{x} + \underline{\lambda}^T (A \underline{x} + u B \underline{x} + \underline{b}) \quad , \quad (2.15)$$

then (a) $\underline{\lambda}(t)$ satisfies

$$\dot{\underline{\lambda}} = - \frac{\partial H}{\partial \underline{x}} \equiv -2C \underline{x} - A^T \underline{\lambda} - u B^T \underline{\lambda} \quad . \quad (2.16)$$

with either (i) $\underline{\lambda}(T) = \underline{0}$ (2.17)

or (ii) $\underline{\lambda}(0) = \underline{\lambda}(T)$, (2.18)

corresponding to conditions (i) and (ii) in (2.12)-(2.13),

and (b) $H(\underline{x}, u, \underline{\lambda}) = \max_{\tilde{u} \in [0, 1]} H(\underline{x}, \tilde{u}, \underline{\lambda})$, $\forall t \in [0, T]$. (2.19)

Condition (b) implies that the optimal control, u , must satisfy

$$u \underline{\lambda}^T B \underline{x} = \max_{\tilde{u} \in [0, 1]} \tilde{u} \underline{\lambda}^T B \underline{x} \quad , \quad (2.20)$$

where $\underline{\lambda} = (\lambda_1, \lambda_2)^T$, and hence

$$u = \begin{cases} 1 & \text{if } \underline{\lambda}^T B \underline{x} > 0 \\ 0 & \text{if } \underline{\lambda}^T B \underline{x} \leq 0 \end{cases} \quad . \quad (2.21)$$

Thus the optimal control takes values only on the boundaries of the admissible interval $[0,1]$ - and it is therefore "bang-bang" as required.

A difficulty arises if

$$H_u = \lambda^T Bx = -\lambda_2 Gv \equiv 0 \quad (2.22)$$

over any finite sub-interval of $[0,T]$, called a singular arc.

There are two cases for H_u to be identically zero:

either (a) $v \equiv 0$ (2.23)

or (b) $\lambda_2 \equiv 0$. (2.24)

For case (a), differentiating (2.23) and using the state equation (2.9), we have the condition

$$\dot{f} = p^2 x = [(k+c) + uG]v \equiv 0$$

along a singular arc. Differentiating again, and applying assumption (2.23), we obtain the condition

$$\ddot{f} \equiv 0, \quad (2.25)$$

necessary along a singular arc. For a harmonic forcing function however, \dot{f} is only zero at isolated points, so that (2.25) cannot be satisfied and, hence, case (a) can be dismissed. An anomaly seems to arise here - the formulation of the original problem requires that the device should be clamped during controlled intervals of time - that is, that $v \equiv 0$ when $u = 1$, but we have proved here that $v \neq 0$ over any finite sub-interval of $[0,T]$. However, in the mathematical model, the clamping of the device is represented by the application of an additional damping force of large magnitude. This modelling is only precise if the damping coefficient, G , is infinite, and for any value of G less than infinity the device velocity will be non-zero over controlled intervals. There is, therefore, no contradiction in this proof.

For case (b) we utilise the additional condition (Bryson and Ho [1975])

$$-\frac{\partial}{\partial u} \left(\frac{d^2}{dt^2} \lambda^T B \underline{x} \right) \leq 0 \quad (2.26)$$

necessary for $E(u)$ to be maximised. Differentiating H_u twice with respect to t , using the assumption (2.24), and the state and adjoint equations (2.11 and 2.16 respectively), we find that

$$\frac{d^2}{dt^2} H_u = 2cGv (f - p^2x - [(k+c) + uG]v),$$

and thus, for our problem

$$-\frac{\partial}{\partial u} \left(\frac{d^2}{dt^2} \lambda^T B \underline{x} \right) = 2cG^2 v^2 \geq 0$$

along a singular arc if (2.24) holds. This contradicts (2.26) if $v \neq 0$, and it follows that no singular arc may exist in the optimal solution.

2.3 Existence of the Optimal

Existence of an optimal solution to problem (2.10)-(2.14) can be proved as follows, using Theorem 1 in Chapter 1 of Lee and Markus [1967].

Theorem

Given the control problem consisting of the following:

(a) a differential system

$$\dot{x}_i(t) = g_i(\underline{x}, t) + \sum_{j=1}^m h_{ij}(\underline{x}, t) u_j(t)$$

for $i = 1, \dots, n$.

With

$$g_i(\underline{x}, t), \quad h_{ij}(\underline{x}, t) \quad \text{and} \quad \frac{\partial g_i}{\partial x_k}(\underline{x}, t), \quad \frac{\partial h_{ij}}{\partial x_k}(\underline{x}, t)$$

- for $k = 1, \dots, n$, all continuous in $\mathbb{R}^n \times \mathbb{R}$;
- (b) a non-empty, convex and (sequentially) compact restraint set $\Omega \subset \mathbb{R}^p$;
- (c) the initial point $\underline{x}_0 \in \mathbb{R}^n$ and the compact target set $S(t) \subset \mathbb{R}^n$;
- (d) the cost functional

$$C(u) = \int_0^T [g_0(\underline{x}, t) + \sum_{j=1}^m h_{0j}(\underline{x}, t) u_j(t)] dt$$

where $g_0(\underline{x}, t)$ and $h_{0j}(\underline{x}, t)$ are continuous on $\mathbb{R}^n \times \mathbb{R}$, then there exists an optimal control, u , if the state \underline{x} is uniformly bounded over the set of admissible controls for all $t \in [0, T]$; that is, if

$$\max_{t \in [0, T]} |\underline{x}(t)| \leq R < \infty, \quad (2.27)$$

where

$$|\underline{x}(t)| = \left(\sum_{i=1}^n x_i^2(t) \right)^{\frac{1}{2}}.$$

It is clear that the problem defined by (2.10)-(2.12) and (2.14) satisfies the conditions (a)-(d) of the theorem, since the state equations (2.11) are linear in \underline{x} , and u . It remains to prove that the state, \underline{x} , satisfies condition (2.27). Integrating both sides of the differential equation (2.11) yields

$$\underline{x}(t) = \int_0^t \{A\underline{x}(s) + u(s)B\underline{x}(s) + \underline{b}(s)\} ds, \quad (2.28)$$

so that

$$|\underline{x}(t)| \leq \int_0^t |A\underline{x}(s) + u(s)B\underline{x}(s) + \underline{b}(s)| ds.$$

Employing the bound on the control, $|u(s)| \leq 1$, and setting

$$Q = \max \{ (|A| + |B|), \max_s |\underline{b}(s)| \} > 0,$$

where $|A|$ is the matrix norm subordinate to the vector norm $|\underline{x}(t)|$, we may write

$$|\underline{x}(t)| \leq Q \int_0^t |\underline{x}(s)| + 1 \, ds = Qt + \int_0^t Q|\underline{x}(s)| \, ds .$$

Applying Gronwall's inequality (Curtain and Pritchard [1977]), we obtain

$$|\underline{x}(t)| \leq e^{Qt}, \quad (2.29)$$

and hence

$$\max_{t \in [0, T]} |\underline{x}(t)| \leq e^{QT} = R < \infty \quad (2.30)$$

and existence of an optimal solution follows.

2.4 Lagrange Formulation

We have shown in the previous section that the solution to the optimal control problem (2.10)-(2.14) is a piecewise constant control u , satisfying a non-linear two-point boundary value problem defined by (2.11) and (2.12) or (2.13) and (2.16) with (2.17) or (2.18), together with (2.21). The solution can be obtained by an iterative process which is described in the following section. In order to establish the convergence of this process, we investigate the Lagrangian functional associated with the problem and find an alternative derivation of the necessary condition (2.21), for the optimal.

The Lagrange functional associated with problem (2.10)-(2.14) is defined by

$$L(u) = E(u) + \int_0^T \underline{\lambda}^T \cdot (A\underline{x} + uB\underline{x} + \underline{b} - \dot{\underline{x}}) dt, \quad (2.31)$$

where $\underline{\lambda}(t) \in \mathbb{R}^2$ is a continuous vector of Lagrange multipliers. We examine the variation in the functional L for any admissible variation, δu , in the control u . We define the "first variation", $\delta L(u, \delta u)$, of the functional L to be linear in δu , and such that

$$L(u + \delta u) - L(u) = \delta L(u, \delta u) + O(|\delta u|).$$

It is well known [Gelfand and Fomin (1963)] that for an admissible control, u , to be optimal, it is necessary that δL be negative for all admissible variations in the control; that is,

$$\delta L(u, \omega - u) \leq 0 \quad \forall \omega \in D. \quad (2.32)$$

If we define the difference between the states corresponding to admissible controls u and $\omega = u + \delta u$, as $\delta \underline{x} = \underline{x}(\omega) - \underline{x}(u)$, then, since matrix C is symmetric, the variation in the functional is given by

$$\begin{aligned} L(\omega) - L(u) &= \int_0^T \delta \underline{x}^T C \delta \underline{x} + \delta \underline{x}^T (2C\underline{x}(u)) \\ &+ \underline{\lambda}^T \{A\delta \underline{x} + uB\delta \underline{x} + \delta uB\underline{x}(u) + \delta uB\delta \underline{x} - \delta \dot{\underline{x}}\} dt. \end{aligned} \quad (2.33)$$

Using integration by parts, and letting $\underline{\lambda}$ be a continuous function satisfying the adjoint equation (2.16) and transversality condition (2.17 or 2.18), we obtain

$$\begin{aligned} L(\omega) - L(u) &= \int_0^T \delta u \underline{\lambda}^T B \underline{x}(u) dt \\ &+ \int_0^T \delta \underline{x}^T C \delta \underline{x} dt \\ &+ \int_0^T \delta u \underline{\lambda}^T B \delta \underline{x} dt. \end{aligned} \quad (2.34)$$

The first variation, $\delta L(u, \delta u)$, of the functional is, therefore, given by

$$\delta L(u, \delta u) = \int_0^T \delta u \underline{\lambda}^T B \underline{x}(u) dt,$$

and hence for an admissible control, u , to be optimal, it is necessary that

$$\int_0^T (\omega - u) \underline{\lambda}^T B \underline{x}(u) dt \leq 0 \quad \forall \omega \in D. \quad (2.35)$$

It is clear, therefore, that an optimal control u must take the piecewise

constant form, (2.21), previously derived.

Thus, we have now shown that an optimal solution to our problem exists and we have derived necessary conditions for such a solution to satisfy. In the following section we describe the numerical methods used to determine the solution.

- Step 4 Evaluate $E^i := \int_0^T \underline{x}^{iT} C \underline{x}^i dt.$
- Step 5 If $|E^i - E^{i-1}| < \text{tol}$, go to step 7.
- Step 6 Set $u^{i+1} := \begin{cases} 1 & \text{if } \underline{\lambda}^{iT} B \underline{x}^i > 0 \\ 0 & \text{otherwise} \end{cases}$
- Set $i := i + 1$
- Go to step 2.
- Step 7 Set $u := u^i$ and STOP.

In the case where boundary conditions (2.13) and (2.17) are imposed and a periodic solution is required, the result is found by repeated integration of the state and adjoint equations over time-intervals of length T , in steps 2 and 3 of the algorithm, until the boundary values of the solutions are equal to within some specified tolerance.

For either set of conditions, the algorithm generates a sequence of admissible controls $\{u^i\}$ and corresponding functionals $E^i = E(u^i)$. The sequence $\{E^i\}$ is bounded since the states \underline{x}^i satisfy (2.30) and therefore, if we can show that the functionals E^i are monotonically non-decreasing, then we can prove (Gruver and Sachs (1980)) that the iteration process described by the algorithm is convergent. Now, it follows from (2.31) that, if $\underline{x}(t)$ satisfies the state equation (2.11) and $\underline{\lambda}(t)$ satisfies the adjoint equation (2.16), then the Lagrangian functional $L(u)$ is equal to the energy functional $E(u)$, and therefore, from (2.34), we have:

$$\begin{aligned}
 E^{i+1} - E^i &= \int_0^T (u^{i+1} - u^i) \underline{\lambda}^{iT} B \underline{x}^i dt \\
 &+ \int_0^T (\underline{x}^{i+1} - \underline{x}^i)^T C (\underline{x}^{i+1} - \underline{x}^i) dt \\
 &+ \int_0^T (u^{i+1} - u^i) \underline{\lambda}^{iT} B (\underline{x}^{i+1} - \underline{x}^i) dt .
 \end{aligned} \tag{3.1}$$

Defining u^{i+1} according to step 6 of algorithm 1, and since the matrix C is positive semi-definite, the first and second terms on the right-hand-side of expression (3.1) are guaranteed non-negative. However, we cannot prove that the third term of the expression is non-negative for all i , and hence convergence of the iteration process defined by algorithm 1 cannot be ensured. Thus we consider an alternative algorithm, employing the conditional gradient method [Gruver and Sachs (1980)]:

Algorithm 2

- Step 1 Set $E^0 := 0$.
- Set $i := 1$
- Choose $u^1 \in D$, piecewise constant, such that $u^1(t) = 0$ or 1 ,
 $\forall t \in [0, T]$.
- Step 2 Solve $\dot{x}^i = Ax^i + u^i B x^i + b$, with boundary conditions (2.12) or (2.13), for $x^i = x(u^i)$.
- Step 3 Solve $\dot{\lambda}^i = -A^T \lambda^i - u^i B^T \lambda^i - 2Cx^i$, with boundary conditions (2.16) or (2.17), for $\lambda^i = \lambda(u^i)$.
- Step 4 Evaluate $E^i := \int_0^T x^{iT} C x^i dt$.
- Step 5 Set $\bar{u}^i := \begin{cases} 1 & \text{if } \lambda^{iT} B x^i > 0, \\ 0 & \text{otherwise} \end{cases}$
- Step 6 If $|E^i - E^{i-1}| < \text{tol}$, go to step 9.
- Step 7 Define, for $\alpha \in [0, 1]$

$$u(\alpha) := u^i + \alpha(\bar{u}^i - u^i)$$
 Find $\alpha^i \in [0, 1]$, such that

$$E(u(\alpha^i)) \geq E(u(\alpha)) \quad \forall \alpha \in [0, 1].$$
- Step 8 Set $u^{i+1} := u(\alpha^i)$.
- Set $i := i + 1$
- Go to step 2.
- Step 9 Set $u := u^i$ and STOP.

Again, if a periodic solution is required, the algorithm must be altered in the same manner as Algorithm 1.

In this algorithm, \bar{u}^i is chosen to satisfy

$$\int_0^T (\bar{u}^i - u^i) \underline{\lambda}^{iT} B \underline{x}^i dt \geq 0, \quad (3.2)$$

so that $(\bar{u}^i - u^i)$ is a direction of non-descent, and if we determine u^{i+1} by a line-search:

$$u^{i+1} = u^i + \alpha^i (\bar{u}^i - u^i), \text{ for some } \alpha^i \in [0,1], \quad (3.3)$$

then $u^{i+1} \in D$. Now

$$\lim_{\alpha \rightarrow 0} \frac{E(u^i + \alpha(\bar{u}^i - u^i)) - E(u^i)}{\alpha} = \int_0^T (\bar{u}^i - u^i) \underline{\lambda}^{iT} B \underline{x}^i dt, \quad (3.4)$$

and hence for some α^i sufficiently small we have, from (3.2), that $E(u^{i+1}) \geq E(u^i)$. It is possible, therefore, to achieve ascent at each iteration, and thus it can be shown that the iteration process described by Algorithm 2 is convergent.

The calculation of the step-length α^i in step 7 of the algorithm is based on the Taylor series expansion of $E(u^{i+1})$ about u^i up to second order, namely

$$\begin{aligned} E(u^i + \alpha(\bar{u}^i - u^i)) &= E(u^i) + \alpha \int_0^T (\bar{u}^i - u^i) \underline{\lambda}^{iT} B \underline{x}^i dt \\ &+ \frac{\alpha^2}{2} \int_0^T 2(\Delta \underline{x}^{iT} C \Delta \underline{x}^i + (\bar{u}^i - u^i) \underline{\lambda}^{iT} B \Delta \underline{x}^i) dt \\ &+ O(\alpha^3), \end{aligned} \quad (3.7)$$

where

$$\Delta \underline{x}^i = \lim_{\Delta \rightarrow 0} \frac{\underline{x}(u^i + \Delta(\bar{u}^i - u^i)) - \underline{x}(u^i)}{\Delta}. \quad (3.8)$$

Thus, to a second order approximation, we wish to find the maximum over $\alpha \in [0,1]$ of

$$E(u^{i+1}) - E(u^i) = \alpha S_1 + \frac{\alpha^2}{2} S_2 = S(\alpha) \quad (3.9)$$

Now, by the definition of \bar{u}^i in step 5 of the algorithm, we have that

$$S_1 = \int_0^T (\bar{u}^i - u^i) \underline{\lambda}^{iT} B \underline{x}^i dt \geq 0 \quad \forall i. \quad (3.10)$$

Hence, in order to maximise $S(\alpha)$ over $\alpha \in [0,1]$, we should define α by

$$\alpha = \begin{cases} 1 & \text{if } S_2 > 0, \\ 1 & \text{if } S_2 < 0 \text{ and } -S_1/S_2 > 1, \\ -S_1/S_2 & \text{if } S_2 < 0 \text{ and } -S_1/S_2 \in [0,1]. \end{cases} \quad (3.11)$$

The term in α^2 in the Taylor expansion (3.7) satisfies

$$\begin{aligned} & \int_0^T 2(\Delta \underline{x}^{iT} C \Delta \underline{x}^i + (\bar{u}^i - u^i) \underline{\lambda}^{iT} B \Delta \underline{x}^i) dt \\ &= \int_0^T (\bar{u}^i - u^i) \cdot \lim_{\Delta \rightarrow 0} \left\{ \frac{\underline{\lambda} (u^i + \Delta (\bar{u}^i - u^i))^T B \underline{x} (u^i + \Delta (\bar{u}^i - u^i)) - \underline{\lambda} (u^i)^T B \underline{x} (u^i)}{\Delta} \right\} dt. \end{aligned} \quad (3.12)$$

Therefore, a good approximation to S_2 is given by

$$S_2 = \frac{\int_0^T (\bar{u}^i - u^i) \cdot \underline{\lambda} (u^i + d(\bar{u}^i - u^i))^T B \underline{x} (u^i + d(\bar{u}^i - u^i)) dt - S_1}{d}, \quad (3.13)$$

for some small value $d > 0$ of Δ , and the accuracy of this approximation may be measured by the known accuracy of the corresponding approximation for S_1 :

$$\int_0^T (\bar{u}^i - u^i) \underline{\lambda}^{iT} B \underline{x}^i dt - \left\{ \frac{E(u^i + d(\bar{u}^i - u^i)) - E(u^i)}{d} \right\}, \quad (3.14)$$

which should be zero to within some small tolerance.

The above analysis also provides an alternative convergence test for the algorithm. Truncating the Taylor series expansion to a first order approximation, we can write

$$E(u^{i+1}) = E(u^i) + \alpha \int_0^T (\bar{u}^i - u^i) \lambda^{iT} B \underline{x}^i dt, \quad (3.15)$$

and hence the halting criterion

$$\left(\int_0^T (\bar{u}^i - u^i) \lambda^{iT} B \underline{x}^i dt \right) / E(u^i) < \text{tol} \quad (3.16)$$

also gives a measure of the convergence of the process. We note that algorithm 2 reduces to algorithm 1 if a step-length $\alpha = 1$ is taken at each iteration.

One drawback of this, second, scheme is that step 7 of the algorithm produces a function $u(\alpha^i)$ which is a convex combination of two controls, and which therefore is not necessarily bang-bang at each iteration. This is not satisfactory since our problem requires a bang-bang solution (although it is possible that the process will converge to a bang-bang control at the optimal).

A third algorithm, which guarantees a bang-bang control at each iteration, is the "Variation of Switching points" method. Again employing the conditional gradient technique [Gruver and Sachs (1980)§7], this is a modified version of algorithm 2 based on the bang-bang principle. The motivation for this method lies in the fact that, due to the nature of our problem, \bar{u}^i is bang-bang at every iteration in algorithm 2. Therefore, if we start the process with a bang-bang control u^1 , and construct the new control by a combination of the switching points of u^i and \bar{u}^i then u^{i+1} will also be bang-bang at every step i :

Algorithm 3

Step 1 Set $E^0 := 0$.

Set $i := 1$.

Choose $u^1 \in D$, piecewise constant, such that $u^1(t) = 0$ or 1 ,
 $\forall t \in [0,1]$.

Set $n := (\text{number of switching points of } u^1) + 1$.

- Step 2 Let u^i be a bang-bang control with m switching points

$$0 \leq t_0^i \leq t_1^i \leq \dots \leq t_m^i \leq t_{m+1}^i = \dots = t_n^i = T,$$
 and $u^i(t) = \frac{1}{2}(1 + (-1)^j)$ for $t \in [t_j^i, t_{j+1}^i)$, $j = 0, \dots, m$.
- Step 3 Solve $\dot{x}^i = Ax^i + u^i Bx^i + \underline{b}$, with boundary conditions (2.12) or (2.13), for $\underline{x}^i = \underline{x}(u^i)$.
- Step 4 Solve $\dot{\lambda}^i = -A^T \lambda^i - u^i B^T \lambda^i - 2Cx^i$, with boundary conditions (2.16) or (2.17) for $\underline{\lambda}^i = \underline{\lambda}(u^i)$.
- Step 5 Evaluate $E^i := \int_0^T \underline{x}^{iT} C \underline{x}^i dt$.
- Step 6 Set $\bar{u}^i := \begin{cases} 1 & \text{if } \underline{\lambda}^{iT} B \underline{x}^i > 0, \\ 0 & \text{otherwise,} \end{cases}$
 where \bar{u}^i has k switching points:

$$0 \leq s_0^i \leq s_1^i \leq \dots \leq s_k^i \leq s_{k+1}^i = \dots = s_n^i = T$$
 (if $k > n$, replace n by $k+1$ and complete the vector of switching points of u^i by $t_j^i = T$ for $j = n+1, \dots, k+1$),
 and $\bar{u}^i(t) = \frac{1}{2}(1 + (-1)^j)$ for $t \in [s_j^i, s_{j+1}^i)$, $j=0, \dots, k$.
- Step 7 If $|E^i - E^{i-1}| < \text{tol}$, go to step 10.
- Step 8 Define, for $\alpha \in [0,1]$,

$$t_j(\alpha) := t_j^i + \alpha(s_j^i - t_j^i) \text{ for } j=0, \dots, n,$$
 and $u(\alpha)(t) = \frac{1}{2}(1 + (-1)^j)$ for $t \in [t_j(\alpha), t_{j+1}(\alpha))$, $j=0, \dots, n$.
 Compute $\alpha^i \in [0,1]$ such that

$$E(u(\alpha^i)) \geq E(u(\alpha)) \quad \forall \alpha \in [0,1].$$
- Step 9 Set $u^{i+1} := u(\alpha^i)$.
 Set $i := i+1$.
 Go to step 2.
- Step 10 Set $u := u^i$ and STOP.

This method can be shown to be convergent [D.Q. Mayne and E. Polak (1975)] and has the advantage over algorithm 2 that a bang-bang control is obtained at each iteration. However, difficulties arise in applying this method to

the discretized problem in cases where step 8 of the algorithm produces a control $u(\alpha)$ with switching points $t_j(\alpha)$ lying between mesh points (see Section 3.2).

We observe that all three algorithms involve the solution of two, first-order, differential equations, and hence - in order to be able to implement the algorithms - it is necessary to discretize the problem. This discretization is described in the following section.

3.2 Discretization of Scheme

In order to discretize the procedure, the interval $[0, T]$ is partitioned into N steps of length $h = T/N$, and solutions are determined at the mesh points $t_j = jh$. The state and adjoint equations are solved using a finite difference technique, and the energy functionals E^i are evaluated using a quadrature rule. The trapezoidal scheme [J.D. Lambert (1973), H.B. Keller (1976)] is chosen to approximate the differential equations on the mesh and the functionals E^i are approximated by the trapezium rule [Johnson and Reiss (1982)]. The state equations are integrated forward from the initial condition $\underline{x}(0) = \underline{x}_0$, and the adjoint equations then integrated backward from the final condition $\underline{\lambda}(T) = \underline{0}$ (or from the current values of $\underline{x}(0)$ and $\underline{\lambda}(T)$ in the case of the periodic problem). The trapezoidal schemes for the state and adjoint equations, (2.11) and (2.16), are given by

$$\begin{aligned} \underline{x}_{-m+1} = \underline{x}_{-m} + \frac{h}{2} \{ & (A\underline{x}_{-m+1} + u_{m+1} B \underline{x}_{-m+1} + \underline{b}_{-m+1}) \\ & + (A\underline{x}_{-m} + u_m B \underline{x}_{-m} + \underline{b}_{-m}) \} \end{aligned} \quad (3.17)$$

and

$$\begin{aligned} \underline{\lambda}_{-m+1} = \underline{\lambda}_{-m} + \frac{h}{2} \{ & (-A^T \underline{\lambda}_{-m+1} - u_{m+1} B^T \underline{\lambda}_{-m+1} - 2C \underline{x}_{-m+1}) \\ & + (-A^T \underline{\lambda}_{-m} - u_m B^T \underline{\lambda}_{-m} - 2C \underline{x}_{-m}) \}, \end{aligned} \quad (3.18)$$

where $\underline{x}_m \approx \underline{x}(mh)$, $\underline{\lambda}_m \approx \underline{\lambda}(mh)$ and $u_m \approx u(mh)$. We observe that since the system equations are linear in \underline{x} and $\underline{\lambda}$, the trapezoidal schemes reduce to one-step explicit methods which can be written as follows:

$$\underline{x}_{m+1} = [I - \frac{h}{2}(A + u_{m+1}B)]^{-1} \{ [I + \frac{h}{2}(A + u_m B)]\underline{x}_m + \frac{h}{2} (b_{m+1} + b_m) \} \quad (3.19)$$

and

$$\underline{\lambda}_m = [I - \frac{h}{2}(A^T + u_m B^T)]^{-1} \{ [I + \frac{h}{2}(A^T + u_{m+1} B^T)]\underline{\lambda}_{m+1} - hC(\underline{x}_{m+1} + \underline{x}_m) \}. \quad (3.20)$$

The differential equations (2.11) and (2.16) are thus solved numerically by the repeated application of the recurrence relations (3.19) (for $m=0, \dots, N-1$) and (3.20) (for $m = N-1, \dots, 0$). Both of these numerical integrations are absolutely stable [J.D. Lambert (1973)] since the eigenvalues of the matrix $(A + uB)$ are given by

$$\mu = -\frac{1}{2} ((k+c) + uG) \{ 1 \pm \sqrt{1 - \left(\frac{2p}{(k+c)+uG} \right)^2} \}, \quad (3.21)$$

where $p^2 > \left(\frac{k+c}{2} \right)^2$ and hence $\text{Re}(\mu) < 0$ as required for absolute stability. From (3.21) we see that the exact solution of the system equations contains an exponentially decaying term

$$x(t) = e^{-Gt} \quad (3.22)$$

On the discrete mesh this term gives rise to a relation

$$x(t_{m+1}) = e^{-Gh} \cdot x(t_m) \quad (3.23)$$

where $t_m = mh$. Numerically, (3.22) is approximated by applying the trapezoidal scheme to the corresponding differential equation

$$\dot{x}(t) = -G x(t) \quad (3.24)$$

giving the recurrence relation

$$x_{m+1} = \left(\frac{1 - h/2 \cdot G}{1 + h/2 \cdot G} \right) x_m \quad (3.25)$$

as an approximation to (3.23). Thus, in order for our numerical approximation to accurately model the physical behaviour of the system, we must ensure that

$$1 - \frac{h}{2} G > 0, \quad (3.26)$$

or

$$N = \frac{T}{h} > \frac{GT}{2} \quad (3.27)$$

The trapezium rule approximates the energy functional by

$$E^i = \frac{h}{2} \{x_0^T C x_0 + x_N^T C x_N + 2 \sum_{m=1}^{N-1} x_m^T C x_m\}, \quad (3.28)$$

and the discrete values of the control are then determined at each iteration by

$$u_m^i = \begin{cases} 1 & \text{if } \lambda_m^{iT} B x_m > 0 \\ 0 & \text{otherwise} \end{cases}, \quad m=0, \dots, N. \quad (3.29)$$

Convergence is at most second order, but high accuracy may be achieved by taking a very small step-length since little storage is required.

Experiments were performed by implementing the above numerical procedures for various choices of the parameters p , K and G , and the forcing function $f(t)$. The results of these tests are described in the next section.

4. RESULTS

Experiments were performed to test the properties of both the physical problem and the mathematical model. For a simple problem - taking a forcing function $f = \sin 2\pi t$ over a time -interval $[0,1]$, and with periodicity enforced - the convergence properties of the numerical procedures were examined. Firstly, the convergence of the different algorithms considered was investigated numerically, and then - for a particular iterative process - convergence of the procedure as a function of both the step-length h and the coefficient G (modelling the clamping of the device in the system equations) was explored. Next, taking values of G and h so as to ensure reasonable accuracy of the numerical technique, the behaviour of the device was studied - for the more realistic, non-periodic, solution; for irregular forcing functions; and for various choices of the spring rate p and time-interval T . In all the experiments, the initial data for the control was taken to be $u^1(t) \equiv 0$ on $[0,T]$, so that the value of the energy functional on the first iteration, E^1 , corresponded to that for the uncontrolled system.

Tables 1(a) and 1(b) illustrate the convergence of the iterative procedures described by algorithms 1 and 2 respectively. Both sets of results are for a simple problem with forcing function $f(t) = \sin 2\pi t$ on a time-interval $[0,1]$ and the following data:

$$p = 12 ; \quad K = c = 1 ; \quad G = 6400 \quad \text{and} \quad N = 3500.$$

The boundary condition (2.13) is imposed - generating a periodic solution. The tables show the behaviour of the switching points - which essentially determine the solution - and the energy functionals, E^i , at a sequence of iterations. Although we are unable to prove convergence of the simplest procedure, algorithm 1 does converge in the majority of cases. However, for more realistic problems, algorithm 2 is more suitable since convergence

is guaranteed. As mentioned in section 3.1, the "Variation of switching points" algorithm (in theory the most suitable of the three methods) does not converge for the cases tested. This may be caused by step 8 of the algorithm producing a control $u(\alpha)$ with switch points $t_j(\alpha)$ lying between the mesh points of the discrete problem. If so, this difficulty might be overcome by using an irregular mesh, updated at each iteration so that all switch points lie on mesh points, and using interpolation to give values of the state and adjoints at the new mesh points. However, this idea has not been examined.

Thus, the most suitable iteration procedure is that given by algorithm 2, and the following experiments all use this method. The drawback of this algorithm, as described in section 3.1, is not a problem in practice: in all the cases considered, algorithm 2 generates a control which becomes bang-bang as the process converges to the optimal. This is illustrated in Figure 1 which shows the graphs of the control, device velocity and incident wave form for the uncontrolled and optimally-controlled systems. In the uncontrolled device, the velocity of the device leads the wave in phase, but with optimal control the velocity is brought into phase with the forcing function - resulting in a fifty-fold increase in energy-capture.

Convergence of the optimal solution generated by this scheme as a function of the time-step h and the clamping coefficient G is illustrated in Tables 2 and 3 respectively. These results are again for the simple periodic problem with $f = \sin 2\pi t$ on $[0,1]$, $p = 12$ and $K = c = 1$.

Values of the energy functional and mid-time displacement at the optimal, and the number of iterations required for convergence are given in Table 2 for a sequence of decreasing step-lengths h . In this case

G takes the value 6400. Therefore, from (3.27), we have the condition $N = T/h > 3200$ for the minimum number of time-steps we may consider. Above this value of N , the method shows convergence of between first and second order.

For a fixed value of N , the behaviour of the solution as G varies between 50 and 6400 is shown in Table 3. Taking $N = 3500$, the upper limit on G according to condition (3.27) is given by $G < 7000$. The solution is described by the energy functional, mid-time displacement and switching points at the optimal. The coefficient G models the device clamping in the system equations - approximating $\dot{x} = 0$ over controlled intervals more accurately as G tends to infinity. The relative accuracy of the solution for $G = 50$ and $G = 6400$ is illustrated in Figure 2 - showing the control, displacement and velocity of the optimally-controlled system. In the latching problem (for G infinite), the velocity is zero and the displacement constant over the controlled ($u=1$) periods of the cycle. Clearly, therefore, taking $G = 50$ does not give sufficient accuracy, whilst $G = 6400$ gives a reasonable approximation to the solution of the latching problem. We observe that the minimum value of G necessary to ensure a reasonable solution is large relative to the magnitude of the other system coefficients ($p = 12, K = c = 1$). From Table 3 we can see that even at $G = 6400$ the energy functional has only converged to 2 decimal places.

From this preliminary analysis we see that for values $G = 6400$ and $N > \frac{GT}{2}$, algorithm 2 converges to a reasonably accurate approximation to the solution of the periodic latching problem for $f = \sin 2\pi t$ on $[0,1]$ with $p = 12$ and $K = c = 1$. The remainder of our experiments use these values of G and N to examine the response of the system to irregular forcing functions and for various choices of the time-interval T and of the ratio of natural device frequency to forcing frequency.

The spring-rating coefficient p in the system equations gives a measure of the natural device frequency. The higher the natural frequency is compared to the forcing frequency, the further the uncontrolled system will be from resonance, and the greater the scope will be for improvement by phase-control. This is illustrated in Figures 3(a) and (b) which show the periodic response over $[0,1]$ to incident monochromatic waves of frequency ω for the optimally-damped ($K=c$), and a sub-optimally damped ($K > c$), system respectively. The energy-capture of the uncontrolled and optimally-controlled systems is compared for ω/p in the range $[0.4,1.4]$. In both cases, the results demonstrate that for incident monochromatic waves of non-resonant frequency, the power output of the device can be significantly improved by phase-control. The effect of this control is shown in Figure 4 for three distinct values of $\omega/p = 1.05, 0.26$ and 0.13 respectively. For a system with lower natural frequency than the incident wave (figure 4(a)), latching control acts to speed up the system. With a natural frequency higher than the incident wave, Figure 4(b) shows that the optimal control slows the device, but for $\omega/p \ll 1$ additional high-frequency harmonics appear in the optimal solution (Figure 4(c)).

The behaviour of the numerical method in computing non-periodic solutions can be seen in Figure 5. The graphs show the uncontrolled and optimally-controlled non-periodic responses to a forcing function $f = \sin 2\pi t$ over 1, 2 and 4 periods of the wave-form respectively. A characteristic of the technique can be seen at the right-hand end of the time-interval in each graph - where the numerical integration procedure gives rise to 'spikes' in the control. However, over a longer time-interval the effect is less significant, and in the periodic solution disappears altogether. Together with Table 4 (which compares the uncontrolled and optimally-controlled

energy functionals for each case) the graphs shown how, as the response is built up from rest, the energy-capture is increased by bringing the velocity into phase with the forcing function. Figure 5 also illustrates how a periodic solution is obtained by the repeated calculation of non-periodic solutions over consecutive unit time-intervals.

The feasibility of phase-control for irregular waves is demonstrated by Table 5, which shows the energy-capture of the uncontrolled and optimally-controlled systems for various irregular-forcing functions. The solutions are non-periodic responses on a time-interval $[0,4]$ for an optimally-damped device ($K = c = 1$) with natural frequency $p = 12$. The exact form of each function is given in Appendix I, along with the mean frequency of each spectrum. The device response to the forcing function f_A is illustrated graphically in Figure 6. From these results we can conclude that for both regular and irregular wave-forms, it is possible to significantly improve device performance by the application of an appropriate control strategy.

i	energy, E^i	switching points at iteration i			
1	.00178				
2	.05110	.00000	.26914	.49971	.76914
40	.06391	.02829	.29057	.52829	.79057
80	.07249	.04629	.30857	.54629	.80857
120	.07724	.05771	.32000	.55771	.82000
160	.08131	.06886	.33143	.56886	.83143
200	.08465	.08029	.34286	.58029	.84286
240	.08718	.09171	.35429	.59171	.85429
280	.8883	.10286	.36571	.60286	.86571
320	.08958	.11371	.37657	.61371	.87657
340	.08964	.11657	.37943	.61657	.87943
341	.08965	.11686	.37943	.61686	.87943
342	.08965	.11686	.37971	.61686	.87971
343	.08965	.11714	.37971	.61714	.87971

Table 1(a) : convergence of Algorithm 1

1	.00178				
2	.05110	.00000	.26914	.49971	.76914
40	.06318	.02686	.28914	.52686	.78914
80	.07211	.04543	.30771	.54543	.80771
120	.07690	.05686	.31914	.55686	.81914
160	.08103	.06800	.33057	.56800	.83057
200	.08443	.07943	.34200	.57943	.84200
240	.08702	.09086	.35343	.59086	.85343
280	.08874	.10200	.36486	.60200	.86486
320	.08957	.11343	.37600	.61343	.87600
343	.08964	.11657	.37943	.61657	.87943
344	.08965	.11686	.37943	.61686	.87943
345	.08965	.11686	.37971	.61686	.87971
346	.08965	.11714	.37971	.61714	.87971

Table 1(b) : convergence of Algorithm 2

Table 2 : convergence of optimal solution with number of time-steps N

N	energy, E^*	$x(0.5)^*$	i^*
1200	.08947	.04881	230
1600	.08952	.04882	249
2000	.08956	.04883	243
2400	.08957	.04883	279
2800	.08958	.04883	319
3200	.08959	.04883	356
3600	.08962	.04883	310
4000	.08965	.04883	301
4400	.08965	.04883	315
4800	.08965	.04883	299

Table 3 : convergence of optimal solution with clamping coefficient, G

G	energy, E^*	$x(0.5)^*$	switching points in $[0, .5]^+$	
			t_1	t_2
50	.00932	.01406	.07714	.33343
100	.01918	.02193	.09600	.35343
200	.03508	.03038	.10657	.36600
400	.05343	.03769	.11257	.37343
800	.06909	.04289	.11514	.37686
1600	.07980	.04609	.11514	.37743
3200	.08614	.04788	.11514	.37771
6400	.08965	.04883	.11714	.37971

⁺ : switching points in $[0.5, 1.0]$ are given by

$$t_3 = t_1 + 0.5$$

$$t_4 = t_2 + 0.5$$

Table 4 : energy-capture of non-periodic system over time-intervals $T = 1, 2$ and 4

T	energy capture		E^*/E^1
	uncontrolled, E^1	opt. controlled, E^*	
1	0.00261	0.00804	3
2	0.00220	0.02042	9
4	0.00197	0.04061	21

Table 5 : energy-capture of non-periodic system with irregular forcing functions, f , for device with natural frequency, $p = 12$.

f	mean freq. $\bar{\omega}$	energy - capture		E^*/E^1
		uncontrolled, E^1	opt. controlled, E^*	
fA	2.5	0.00212	0.01757	8
fB	2.7	0.00086	0.01069	12
fC	2.8	0.00023	0.00593	26
fD	4.7	0.00012	0.00290	25

5. CONCLUSIONS

In this report, we investigate a simple mathematical model of an ocean-wave-energy device and develop techniques, using optimal control theory, for maximising the power output of the system. The energy-extraction problem is formulated as a standard problem of optimal control, and necessary conditions for an optimal solution are derived, showing the optimal control to be non-linear with discontinuities at switches which are to be determined. Existence of such a solution is established, and numerical algorithms for calculating the optimal are developed. The convergence and stability properties of each algorithm are also investigated.

Experiments are performed to test the convergence of the numerical procedures and to examine the improvement in performance possible with phase-control. Convergence to an optimal solution of two of the three algorithms considered is observed (despite having no theoretical proof of convergence for the first method). The third algorithm - in theory the most suitable of the three - proves difficult to apply to the discretized problem.

The second algorithm has convergence guaranteed, and generates an optimal solution with a bang-bang control for all the problems tested. Using this method, convergence of the optimal solution with decreasing mesh-length h and increasing damping coefficient G , is also seen.

Experiments are performed for problems with periodic and non-periodic solutions; regular and irregular forcing functions; and for different choices of both the time-interval T and of the ratio of natural device frequency to forcing frequency. The results demonstrate that device performance can be significantly improved by means of an appropriate control strategy, with the greatest increases in energy-capture being observed for devices operating far from their resonant frequency.

We conclude that phase-control is feasible for the point-absorber for waves in the complete spectrum. However, implementation of such a control mechanism requires forward prediction of the wave-exciting-force in order to compute the optimal control strategy. It is expected that the acting wave-force can be found from measurements of the system states, and that a technique using Kalman filtering to estimate the future behaviour of the wave-force over a short period from its recent history can be applied to obtain the necessary data. Further investigation of these techniques and of more hydrodynamically realistic models is necessary.

6. REFERENCES

- Birkett, N.R.C. : A study of an optimal power extraction problem, M.Sc. Thesis, Univ. of Reading, (1980).
- Birkett, N.R.C., Nichols, N.K. : Optimal control problems in tidal power generation, Dept. of Maths., Univ. of Reading, Num. Anal. Rpt. NA 8/83, (1983).
- Birkett, N.R.C., Count, B.M., Nichols, N.K. : Optimal control problems in tidal power, Water Power and Dam Construction, Jan. (1984), pp. 37-42.
- Budal, K., Falnes, J. : Wave-power conversion by point-absorbers. Norwegian Maritime Research, 6, (1978) (4), 2-11.
- Budal, K. : The Norwegian wave-power buoy project, Proc. of 2nd Int. Symp. on Wave Energy Utilisation, Trondheim, (1982).
- Count, B.M. : On the physics of absorbing energy from ocean waves, Ph.D. Thesis, Univ. of Exeter, (1982).
- Curtain, R.F., Pritchard, A.J. : Functional Analysis in Modern Applied Mathematics, Academic Press, (1977).
- Evans, D.V. : A theory for wave-power absorption by oscillating bodies, J. Fluid Mech., 77, (1976), 1-25.
- Gelfand, I.M., Fomin, S.V. : Calculus of Variations, Prentice-Hall, (1963).
- Gruver, W.A., Sachs, E. : Algorithmic methods in optimal control, Pitman (1980).
- Johnson, L.W., Reiss, R.D. : Numerical Analysis, Addison-Wesley, (1982).
- Keller, H.B. : Numerical Methods for Two Point Boundary Value Problems, Blaisdell, (1976).
- Lambert, J.D. : Computational Methods in Ordinary Differential Equations, John Wiley & Sons, (1973).
- Lee, E.B., Markus, L. : Foundations of Optimal Control Theory, John Wiley & Sons, (1967).
- Mayne, D.Q., Polak, E. : First-order strong variation algorithms for optimal control problems with terminal inequality constraints, J. Optim. Theory Appl, 16 (1975), 303-325.
- Pontryagin, L.S. et al. : The Mathematical Theory of Optimal Processes, John Wiley & Sons, (1962).

APPENDIX I

In the results section of this report, Table 5 and Figure 6 show the system response to various irregular forcing functions of the form

$f(t) = \sum_i A_i \sin(\omega_i t + \phi_i)$. The four different functions considered are tabled below, together with the mean frequency, $\bar{\omega}$, of each spectrum, given by

$$\sum_i (A_i^2 / \omega_i) = (\sum_i A_i^2) / \bar{\omega} \quad (A.1)$$

f	A_i	ω_i	ϕ_i	$\bar{\omega}$
fA	0.2 0.6 0.4 0.4 0.2 1.0	6.2832 3.1416 2.0944 6.2832 3.1416 2.0944	0 0 0 1.5708 1.5708 1.5708	2.4684
fB	0.2 0.6 0.4 0.4 0.2 0.1	6.2832 3.1416 2.0944 6.2832 3.1416 2.0944	0 0 0 1.5708 1.5708 1.5708	2.7180
fC	0.2 0.6 0.4	6.2832 3.1416 2.0944	0 0 0	2.8376
fD	0.04 0.12 0.20 0.28 0.20 0.12 0.04	4.147 4.084 4.398 4.712 5.027 5.341 5.655	2.665 5.052 3.028 2.570 5.202 0.094 3.952	4.692

control

incident wave form

velocity

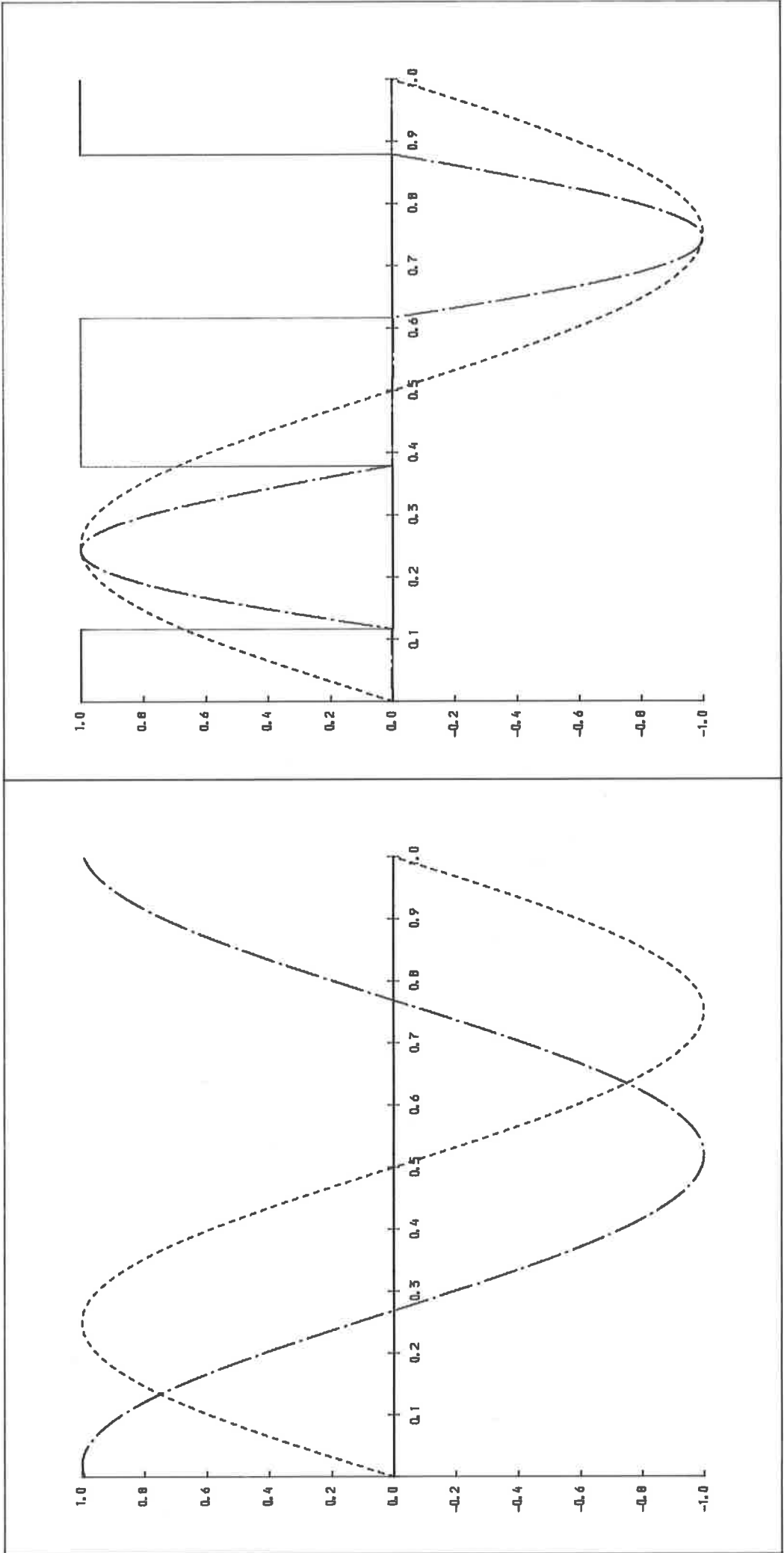


Figure 1(a) : uncontrolled system

Figure 1(b) : optimally-controlled system

control

displacement

velocity

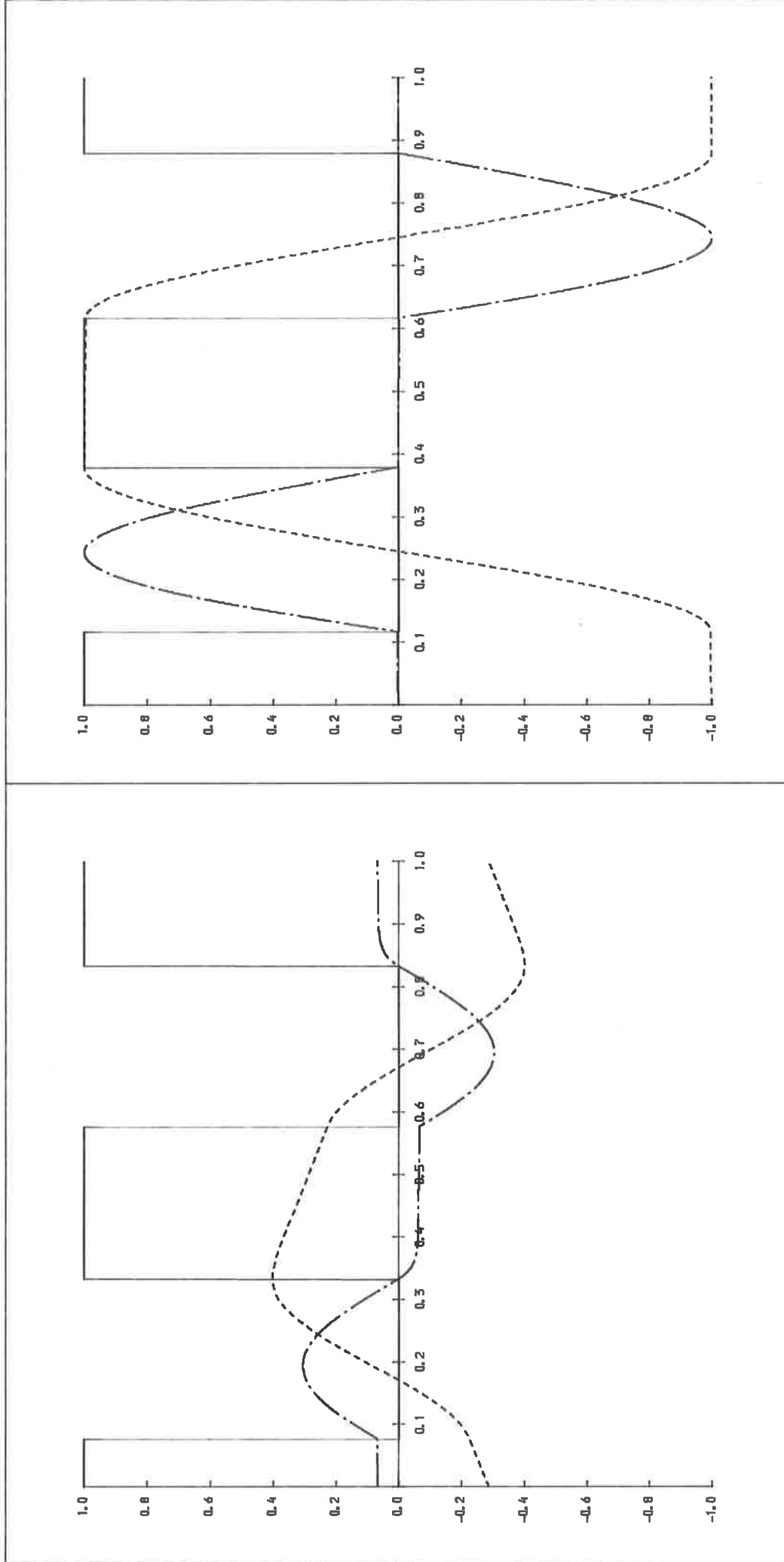


Figure 2(a) : $G=50$

Figure 2(b) : $G=6400$

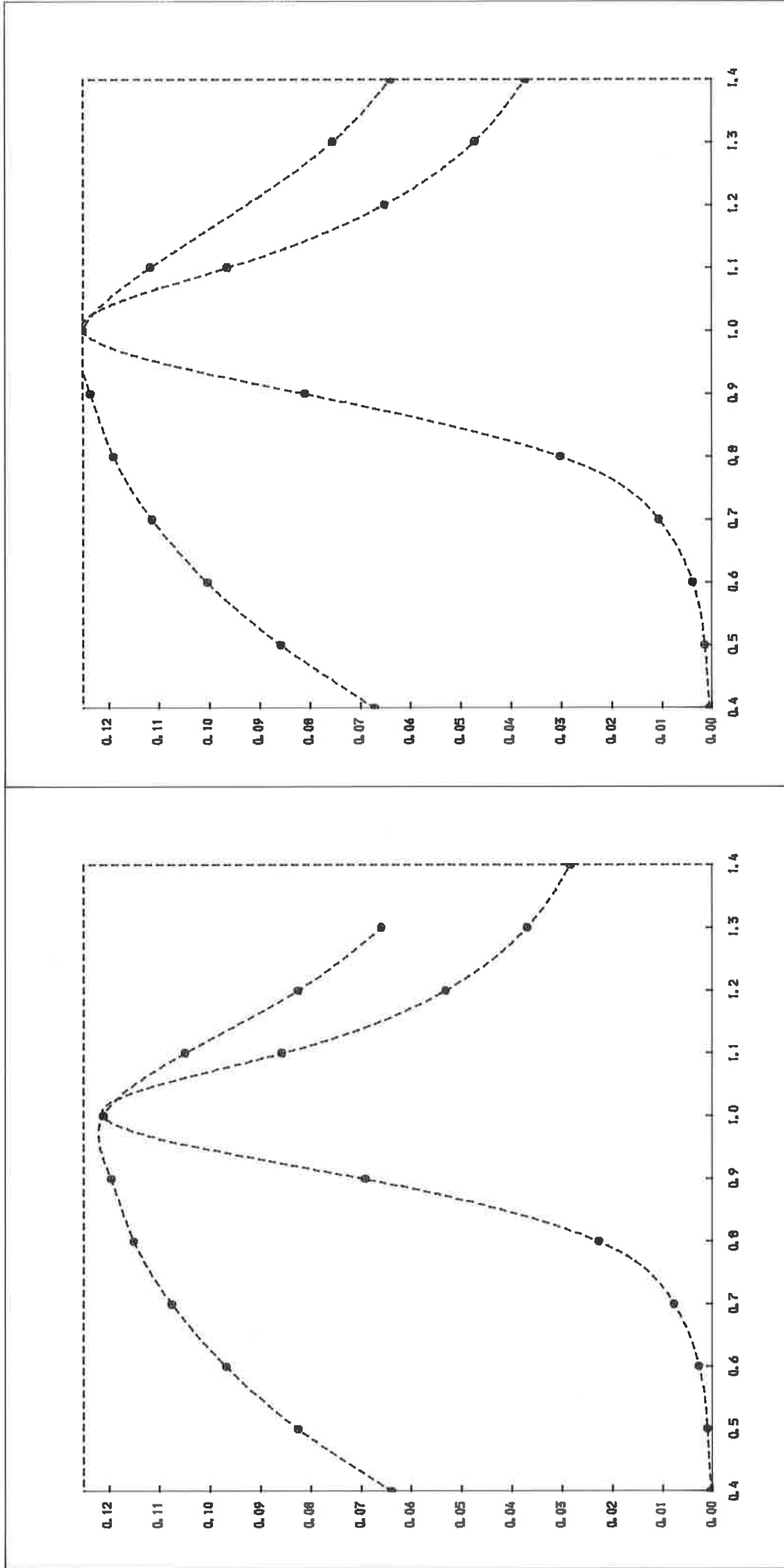


Figure 3(a) : sub-optimally-damped system

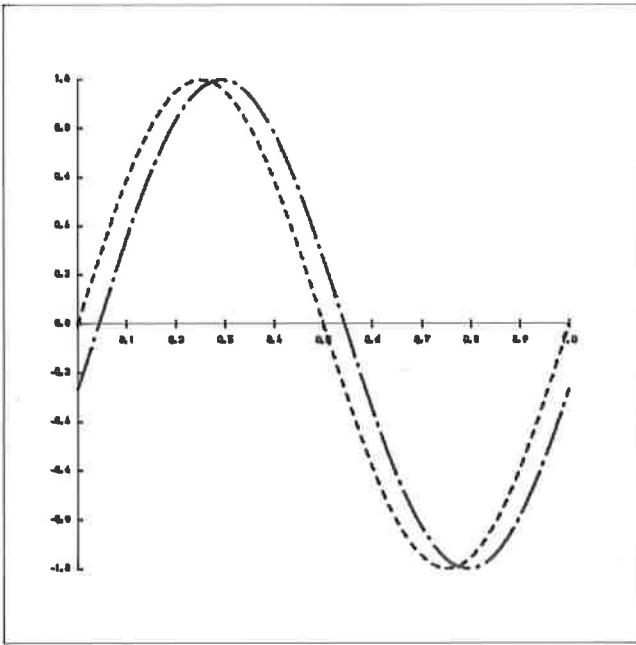
Figure 3(b) : optimally-damped system

Figure 3 : energy-capture of controlled and uncontrolled systems in response to monochromatic incident waves with frequency in the range $\omega \in [0.4p, 1.4p]$

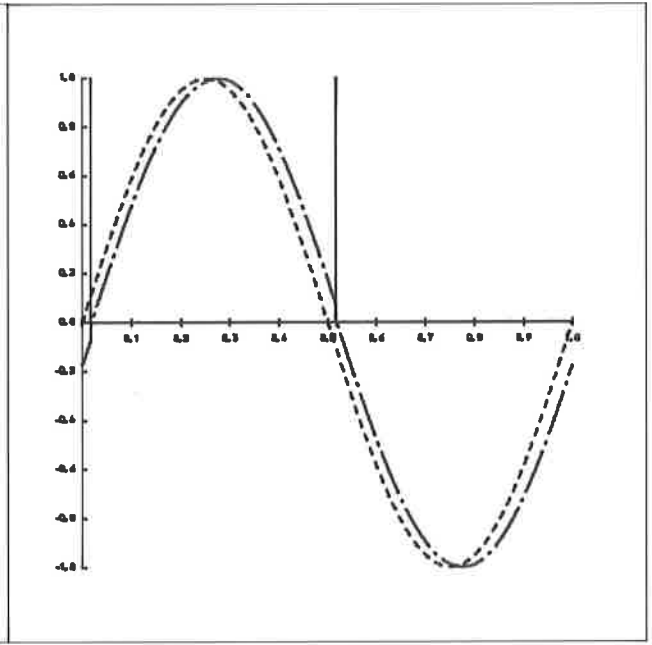
control

incident wave form

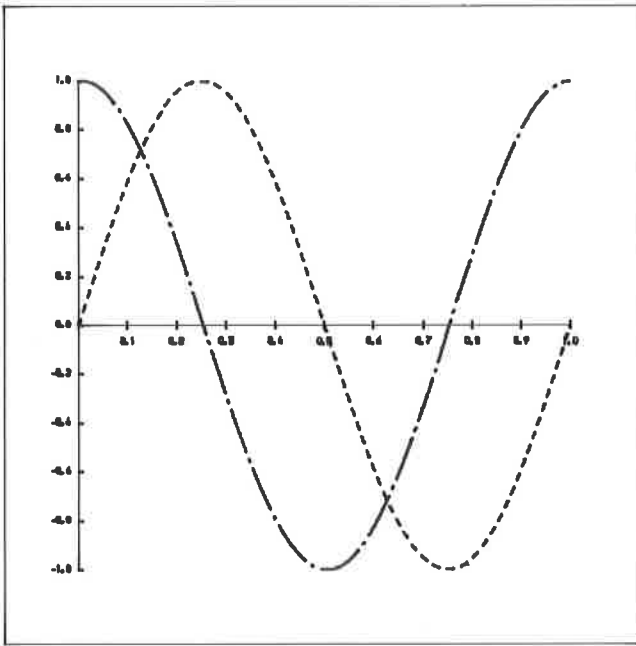
velocity



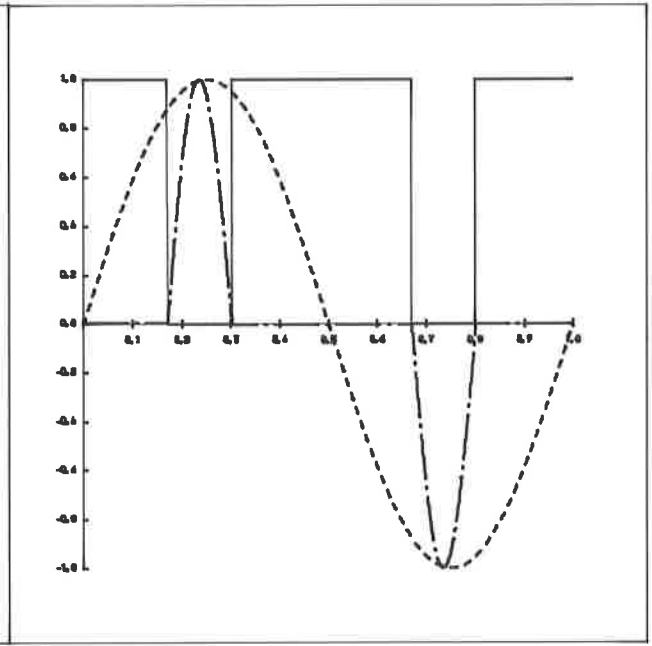
(a) (i) - uncontrolled



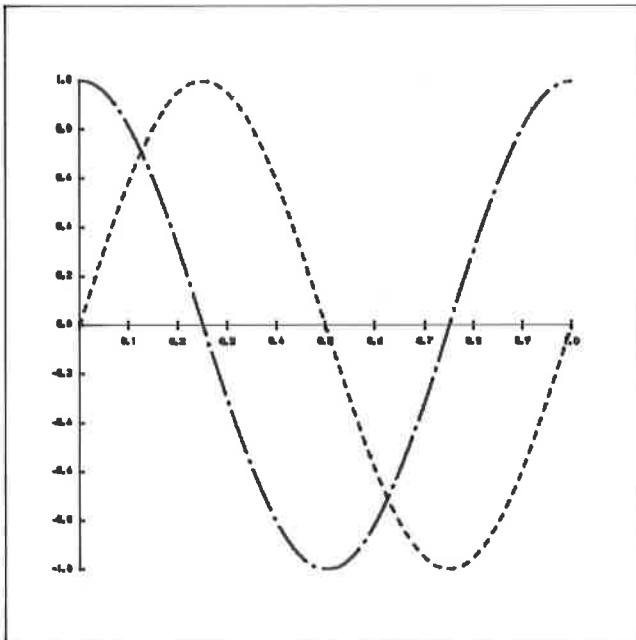
(a) (ii) - controlled



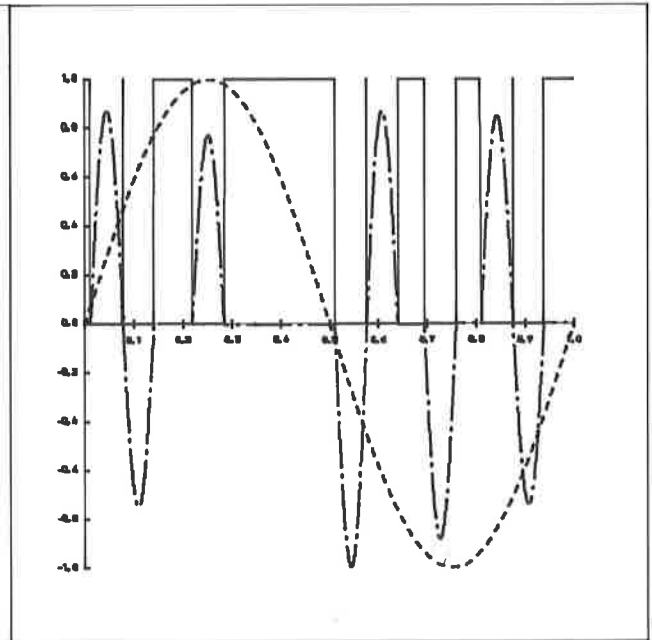
(b) (i) - uncontrolled



(b) (ii) - controlled



(c) (i) - uncontrolled



(c) (ii) - controlled

Figure 4 : response of system with natural frequency (a) $p = 24$, (b) $p = 6$, (c) $p = 48$ to incident wave with frequency $\omega = 2\pi$

—— control - - - - - incident wave form - · - · - · velocity

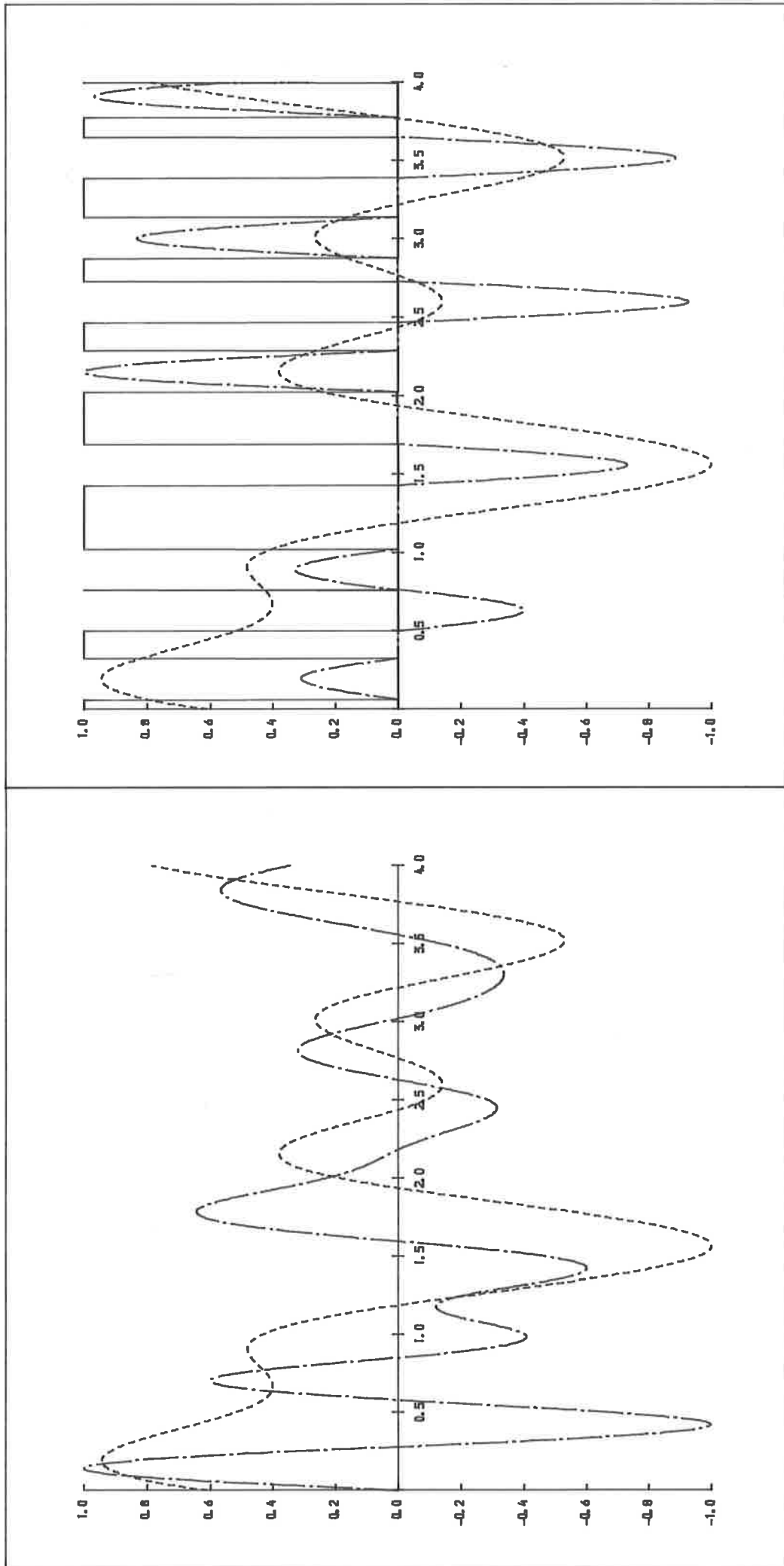


Figure 6(a) : uncontrolled system

Figure 6(b) : optimally controlled system

ACKNOWLEDGEMENTS

This work was carried out with the financial support of the SERC and the Central Electricity Generating Board under the supervision of Dr N.K. Nichols, Dr B.M. Count and Dr D.A.C. Nicol.